The multistatic oceanographic HF radar network in Toulon

Charles-Antoine Guérin, Dylan Dumas, Anthony Gramoulle, Céline Gwenaëlle Quentin, Marc Saillard, A. Molcard

The multistatic oceanographic HF radar network in Toulon

1st Charles-Antoine Guérin
Mediterranean Institute of Oceanography
Univ Toulon, Aix Marseille Univ.,
CNRS/INSU, IRD, MIO UM 110
La Garde, France
guerin@univ-tln.fr

2nd Dylan Dumas
Mediterranean Institute of Oceanography
Univ Toulon, Aix Marseille Univ.,
CNRS/INSU, IRD, MIO UM 110
La Garde, France
dylan.dumas@univ-tln.fr

3rd Anthony Gramoullé
Mediterranean Institute of Oceanography
Univ Toulon, Aix Marseille Univ.,
CNRS/INSU, IRD, MIO UM 110
La Garde, France
anthony.gramoulle@univ-tln.fr

4th Céline Quentin
Mediterranean Institute of Oceanography
Univ Toulon, Aix Marseille Univ.,
CNRS/INSU, IRD, MIO UM 110
La Garde, France
celine.quentin@mio.osupytheas.fr

5th Marc Saillard
Mediterranean Institute of Oceanography
Univ Toulon, Aix Marseille Univ.,
CNRS/INSU, IRD, MIO UM 110
La Garde, France
marc.saillard@univ-tln.fr

6th Anne Molcard
Mediterranean Institute of Oceanography
Univ Toulon, Aix Marseille Univ.,
CNRS/INSU, IRD, MIO UM 110
La Garde, France
anne.molcard@univ-tln.fr

***Abstract*—The Mediterranean Institute of Oceanography (MIO) and the University of Toulon operate a HF radar network for sea surface current monitoring in the Mediterranean Sea. This radar system was recently upgraded in the framework of the EU Interreg project SICOMAR-PLUS and is now running in a multistatic mode with 2 TX and 2 RX located on three distant sites. This original configuration combined with some innovations in the radar data processing allows for an increased coverage and improved spatiotemporal resolution of surface currents maps in the coastal region of Toulon. We present the main characteristics of this updated HF radar network together with a rapid overview of the specific processing techniques it requires. Preliminary results showing the potential performances of this network are presented.**

***Index Terms*—HF radar, surface current, multistatic**

I. Introduction

The Mediterranean Institute of Oceanography (MIO) and the University of Toulon have been operating for one decade a network of HF radar systems (manufactured by WERA Helzel Messtecknik) for the daily monitoring of surface currents in the coastal area of Toulon (e.g. [1], [2]). This network is being currently upgraded in the framework of the EU Interreg Maritimo program SICOMAR-PLUS and, as of January 1st, 2019, it is maintained operational by the company *Degréane Horizon*. The originality of this HF radar network is that it is fully multistatic, that is with several separated emitters and receivers. This non-standard configuration has been imposed by the complex topography of the area (shadowing effects of several islands near the coast) and the reduced available space on the radar sites (which does not allow for a sufficient isolation between the emitting and receiving antennas). Albeit more complex to operate, the multistatic configuration provides richer information from an oceanographic point of view (increased coverage at sea and augmented number of projected surface current directions for the cartography).

The principle of surface current extraction from HF radar has been known for at least 4 decades since the pioneering works of Crombie [3] and Barrick [4]; we refer to e.g. [5], [6] for reviews of the methods and applications. The main physical principle underlying this detection is the presence of a resonant wave at half the radar wavelength (λ/2), referred to as the Bragg wave. The dominant contribution of this wave to the backscattered radar signal produces a very marked peak in the Doppler spectrum at the so-called Bragg frequency, $f_B = \sqrt{g/\pi\lambda}$, inferred from the dispersion relationship of the resonant gravity wave. Any observed shift of the main Doppler peak with respect to the Bragg frequency is attributed to the translational effect of a surface current; the magnitude of this shift can be converted into an algebraic value of the radial speed (i.e., projected along the radar line of sight) of the surface current. A radial surface current map can thus be obtained with one monostatic radar after range and azimuthal cell discrimination. Range resolution is obtained by binning the 2-way travel time at the hardware level while azimuthal resolution requires numerical post-processing of the complex time series (I and Q channels) recorded on the set of antennas. The bearing angle of the radar cells is usually determined by a classical beam-forming technique for extended linear receive arrays and a direction finding technique based on the subspace projection algorithms for compact receive antennas.

Today, there are about 400 shore-based stations around the world collecting routinely surface currents along the coasts based on this methodology. The vast majority of these installations operate in the monostatic mode with commercial software. The bistatic geometry [7] is slightly more complicated in as much as the iso-range radar cells follow ellipses with focii at the emitter and receiver, the Bragg frequency varies with the cell coordinates and the Doppler shift measurement relates to the projection of the surface current vector onto the local normal to the ellipse, a component which we refer to as the "elliptical" radial (fig. 1). Due to the bistatic geometry and also due to the necessity to cope with several simultaneous emitters the multistatic configuration requires specific processing techniques, which have been developed at the laboratory. Another specificity of our approach is to apply an improved direction finding (rather than beam forming) algorithm to noncompact arrays (both linear and nonlinear) of receive antennas. This allowed us to obtain high-resolution current maps at a fast temporal sampling rate (20 min).

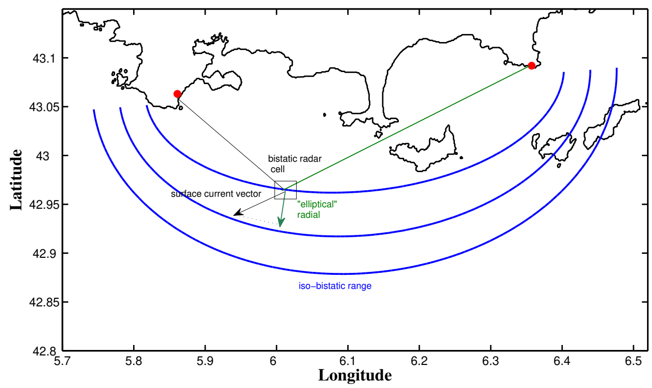

Fig. 1. Bistatic geometry for the HF radar surface current inversion.

II. Description of the multistatic HF radar network

The HF radar network is composed of 2 transmitters (TX) and 2 receivers (RX) located on three distant sites, referred to as POR, PEY and BEN (Fig. 2). A standalone emitter with carrier frequency $f = 16.150$ MHz (wavelength $\lambda = 18.54$ m) is located on Porquerolles island ((POR, $42°59'01.1"N$ $6°12'21.7"E$) 27 km South-East of Toulon; its single, nondirectional, emitting antenna illuminates a wide sea area to the South. A first receiver is located at Cap Bénat ($43°05'21.4"N$ $6°21'46.9"E$, altitude 175 m) 35 km East of Toulon (BEN), with a regular linear array of 12 receiving active antennas (70 deg from North, anticlockwise) with $0.45\ \lambda$ spacing. The second emitter and receiver are located at Fort Peyras (PEY) about 8 km South West of Toulon ($43°03'48.7"N$ $5°51'39.3"E$, altitude 165 m). Due to the lack of space on the site and the specific topography, only 8 receiving passive antennas could be installed in a non-regular arrangement, describing a zig-zag about a main direction oriented 5 deg from North anticlockwise (a solution was recently found to place a regular array of 12 active antennas, which will be installed by the summer 2019). Two emitting antennas were sited a few tens of meter away from the receiving antennas. The direct coupling was minimized by orienting the null of the 2-antenna array toward the main direction of the receiving array and by taking advantage of the natural sheltering effect of the site topography.

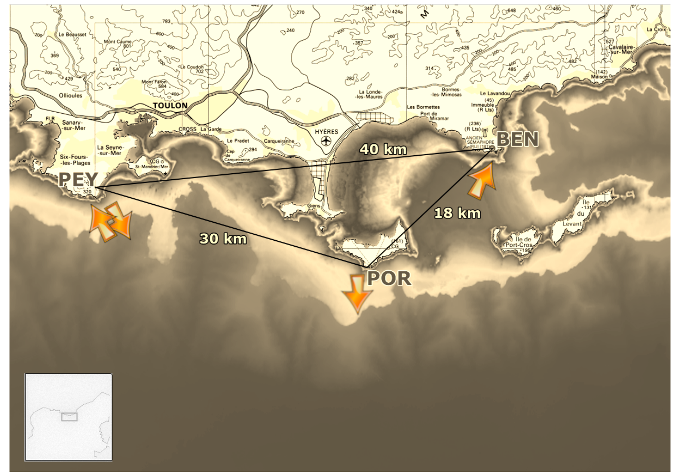

Fig. 2. The three HF radar sites in the region of Toulon: 1) Fort Peyras (TX/RX, "PEY"); 2) Cap Bénat (RX, "BEN"); 3) Porquerolles (TX, "POR")

III. Processing of the radar signals

A. Bistatic range resolution with two emitters

The two emitters POR and PEY send continuous chirp ramps of duration 0.26 seconds within a frequency band of 100 kHz around the same central frequency $f = 16.150$ MHz, allowing for a 1.5 km range resolution. In the standard frequency-modulated continuous wave (FMCW) HF radar technology, the range gating is obtained by binning the received signal in frequency shifts [8]. In order for the receivers to discriminate the signal scattered from the two different sources, the two emitting central frequencies are offset by a multiple of a frequency bin, namely a small value 246 Hz corresponding to the first 64 range cells. Hence a simultaneous range processing of the received signal according to the 2 different emitters can be obtained by allocating the first 64 range cells to one emitter and the next 64 range cells to the other emitter. It is thus assumed (and verified) that the scattered signal from the first emitter is attenuated beyond the 64th range cell (96 km) so that it does not interfer with the first range cells of the second emitter.

Fig. 3 and 4 show typical range-Doppler maps obtained by processing the range resolved temporal signal received on a single antenna in Cap Bénat and Peyras, respectively. The first "floor" corresponds to the bistatic sea echo from "Pey" while the second floor is the bistatic return from POR. Note that the present combination of 2 TX and 2 RX leads to 3 bistatic pairs (POR-BEN, POR-PEY, PEY-BEN) and 1 monostatic pair (PEY-PEY) of TX/RX. In the traditional monostatic configuration, it is well-known that the main feature of the range-Doppler map is the so-called first-order Bragg line, which is a pronounced resonant "Bragg" Doppler frequency at $f_B = 0.41$ Hz regardless of the range; this marked line is visible on PEY-PEY range-Doppler map (first floor of Fig. 4). In the less usual bistatic configuration, the resonant Bragg frequency (hence the position of Bragg lines) is range dependent with a typical U-shape signature on the range-Doppler maps. Another peculiarity of this geometry is an offset in range for the first cells showing Bragg lines. This offset corresponds to half the straight distance between emitter and receiver, which is the minimum bistatic range for the signal scattered from the sea surface.

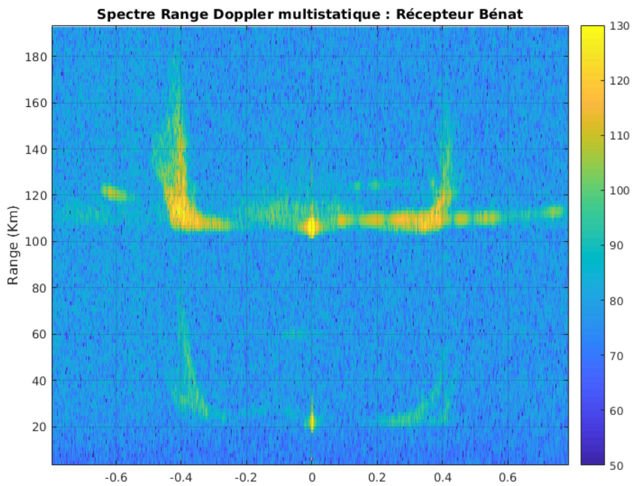

Fig. 3. A multistatic range-Doppler map seen from Cap Bénat

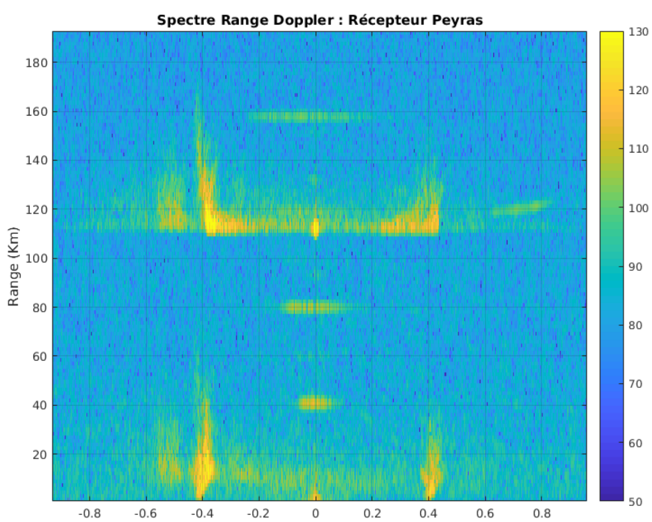

Fig. 4. A multistatic range-Doppler map seen from Fort Peyras

B. Azimuthal processing

The critical step in processing HF radar data for producing current maps is the azimuthal discrimination of the received signal. For linear arrays of antennas, this is usually done with a Beam Forming (BF) technique which allows to steer the bearing angle by adjusting numerically the relative phase shifts of the antenna signals. This makes it possible to sweep continuously the angular sector covered by the radar. However, the resulting azimuthal accuracy depends on the array extension. From classical antenna theory it is well known that the half-power width of the array factor is λ/L in the central direction (that is, perpendicular to the array), where L is the array length. For a typical $\lambda/2$ antenna spacing, this implies about 10 deg azimuthal resolution with a 12-antenna array and 8 deg with a 16-antenna array. However, the azimuthal resolution deteriorates significantly as the steering angle deviates from the central direction (by about a factor 2 at ± 60 degrees). The beam forming technique does not hold for compact antenna systems; these make instead use of a Direction Finding (DF) technique applied to each Doppler ray of the omnidirectional Doppler spectrum (that is, azimuthally nonresolved) measured on every single antenna. The accurate identification of a source direction for every possible shifted Bragg peak (hence every possible elliptical radial surface current) is made with help of subspace-based methods [9], [10]. This powerful technique provides high-resolution maps. However, it suffers from two important shortcomings. First, a large observation time (at least one hour) is needed to estimate accurately the statistical covariance matrix of antenna signals, which is at the core of this algorithm; second, the resulting maps can be very lacunary, as some radar cells might be never allocated in the direction finding process. To bypass the limitations of BF with short receiving arrays (8 and 12 antennas, respectively) and to avoid at the same time the weak points of DF (long observation time, lacunary maps), we designed an improved DF technique for extended linear (or quasi-linear) arrays. We were thus able to produce high-resolution elliptical radial current maps with full coverage and at the temporal rate of one hour. An example of such maps is shown in Fig. 5, where the four available elliptical radials are shown, according to the possible combinations TX/RX.

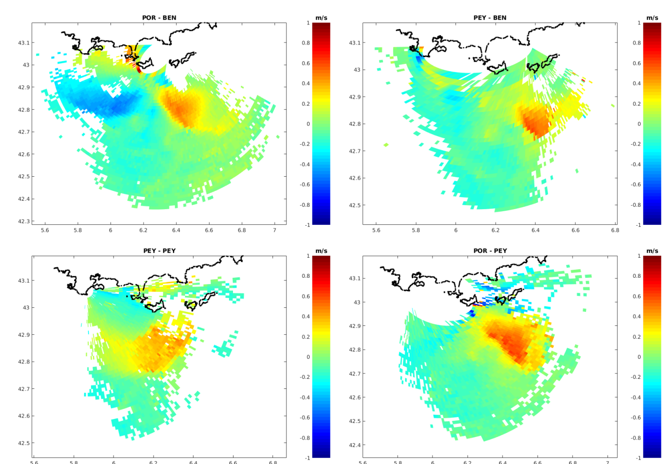

Fig. 5. Four simultaneous elliptical radials maps resulting from a 1 hour observation time on February 4, 2019 (14:00-15:00 UTC).

C. RFI processing

Another challenging aspect in HF radar data processing is the ability to process the signal in the presence of strong Radio

Frequency Interferences (RFI). These are external anthropic sources in the frequency band of the emitter which can severely corrupt the received sea echo at all range gates and hinder the estimation of surface current. Their typical signature is one or a set of marked vertical lines in the range-Doppler map (Fig. 6). Classical mitigation of RFI sources relies on dynamical emitting frequency adjustments ([11], [12]) and recording of the "negative" time-delays (corresponding to the negative frequencies in the FFT range-gating operation) into a so-called "RFI file" [8]. In bistatic mode where the remote TX and RX systems must work coherently, the "listen before talk" technique does not apply but we found an efficient way to clean the range-resolved radar signal using the RFI files. Fig. 6 shows an example of a strongly corrupted file before and after applying the denoising technique.

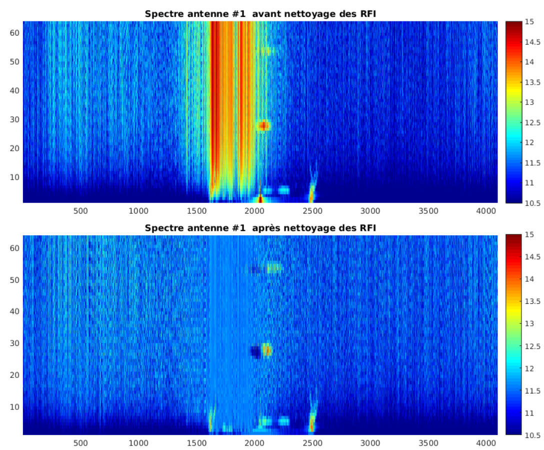

Fig. 6. Range-Doppler maps before and after denoising in a corrupted case.

IV. Reconstruction of oceanic surface currents vectors

Application of the aforementioned processing steps leads to 4 elliptical radial maps which are used to produce a vector current map. For this, all available current projections entering in every chosen grid cell (from 2 to 4 according to the location) are combined into a single vector using a least-square minimization. To reduce reconstruction errors only projected directions differing by an angle of at least 20 degrees are retained. Fig. 7 shows the reconstructed vector current map according to the four bistatic projections given in Fig. 5. A comparison with the maps obtained through a 6 hours average around the same period is displayed in Fig. 8; the consistent features observed over this longer time scale confirm the relevance of the short time observation. The expected strong signature of the Ligurian Current [13] is clearly visible. Note that the radar coverage extends up to about 70 km South off the coast of Toulon with a maximum lateral extension of about 40 km. It is also important to note that at this stage we did not yet apply any post-processing techniques which are usually employed to "clean" the geophysical data. The present surface current map is therefore a "Level 0" radar product, contrarily to the standard higher-level data processing where statistical tools are used to remove the outliers and dubious values, fill the gaps and smooth the data.

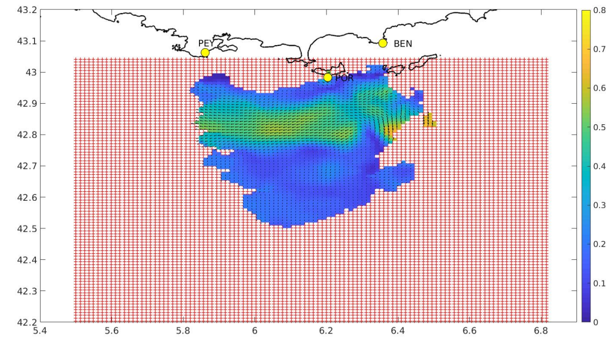

Fig. 7. Recombined elliptical radials of the surface current for a one hour observation on February 4, 2019 (14:00-15:00 UTC). Only the area with 4 simultaneous existing radials are reconstructed. The colorscale is in m/s.

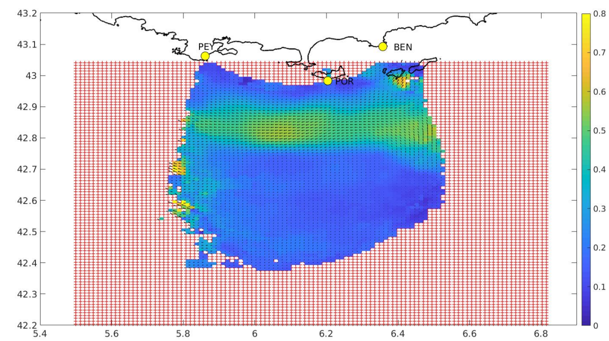

Fig. 8. Same as Fig. 7 for a 27 hours observation on February 3-4, 2019 (from 21:00 UTC).

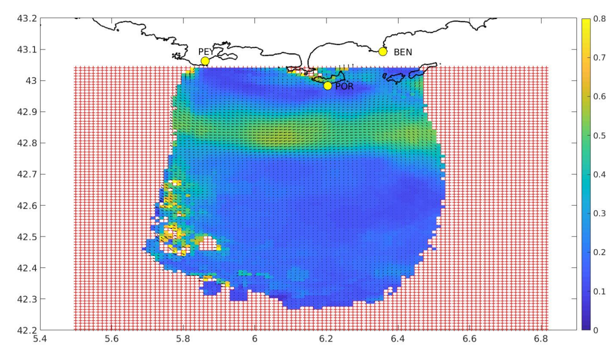

Fig. 9. Same as Fig. 8 with only 2 (at least) simultaneous radials required.

We have presented the first results pertaining to the upgraded multistatic HF radar network in the area of Toulon.

By taking full advantage of the bistatic geometry and by improving the data processing techniques, we have obtained high-resolution vector maps of the regional surface currents in a wide area at an hourly rate. The RX site in Fort Peyras will soon be further upgraded to extend the nonlinear 8-antenna array to a linear 12-antenna array and a long-term systematic study will be presented in the future.

Acknowledgment

The upgrade and maintenance of the WERA HF radar system in Toulon as well as one of the authors (Anthony Gramoullé) have been funded by the EU Interreg program SICOMAR-PLUS. We acknowledge the University of Toulon for granting a one-year research support to this project (Dylan Dumas). We thank B. Zakardjian, D. Mallarino, J-L. Caccia, T. Missamou and J-L. Fuda for helping with the site installation.

References

[1] J. Marmain, P. Forget, and A. Molcard. Characterization of ocean surface current properties from single site HF/VHF radar. *Ocean Dynamics*, 61(11):1967–1979, 2011.

[2] J. Marmain, A. Molcard, P. Forget, A. Barth, and Y. Ourmières. Assimilation of HF radar surface currents to optimize forcing in the northwestern Mediterranean sea. *Nonlinear Processes in Geophysics*, 21(3):659–675, 2014.

[3] D D Crombie. Doppler spectrum of sea echo at 13.56 mc./s. *Nature*, 175(4459):681–682, 1955.

[4] D E Barrick. Remote sensing of sea state by radar. In *Engineering in the Ocean Environment, Ocean 72-IEEE International Conference on*, pages 186–192. IEEE, 1972.

[5] K-W Gurgel, H-H Essen, and SP Kingsley. High-frequency radars: physical limitations and recent developments. *Coastal engineering*, 37(3):201–218, 1999.

[6] J D Paduan and L Washburn. High-frequency radar observations of ocean surface currents. *Annual review of marine science*, 5:115–136, 2013.

[7] S. Grosdidier, P. Forget, Y. Barbin, and C.-A. Guérin. HF bistatic ocean Doppler spectra: Simulation versus experimentation. *IEEE Trans. Geosci. and Remote Sens.*, 52(4):2138–2148, 2014.

[8] K.-W. Gurgel and T. Schlick. Remarks on signal processing in HF radars using FMCW modulation. In *Proc. IRS*, pages 1–5, 2009.

[9] G. Bienvenu and L. Kopp. Optimality of high resolution array processing using the eigensystem approach. *IEEE Transactions on acoustics, speech, and signal processing*, 31(5):1235–1248, 1983.

[10] H. Krim and M. Viberg. Two decades of array signal processing research. *IEEE signal processing magazine*, 1996.

[11] K.-W. Gurgel, Y. Barbin, and T. Schlick. Radio frequency interference suppression techniques in FMCW modulated HF radars. In *OCEANS 2007-Europe*, pages 1–4. IEEE, 2007.

[12] C. R. Merz, Y. Liu, K.-W. Gurgel, L. Petersen, and R. H. Weisberg. *Coastal Ocean Observing System*, chapter Chapter 13 - Effect of Radio Frequency Interference (RFI) Noise Energy on WERA Performance Using the Listen Before Talk Adaptive Noise Procedure on the West Florida Shelf, pages 229–247. Academic Press, 2015.

[13] C. Millot and I. Taupier-Letage. Circulation in the Mediterranean sea. In *The Mediterranean Sea*, pages 29–66. Springer, 2005.